GENERATION AND KINEMATICS OF THE INTERNAL TIDE IN THE STRAIT OF GIBRALTAR

N. A. BRAY[1]
C. D. WINANT[1]
T. H. KINDER[2]
J. CANDELA[1]

[1] Center for Coastal Studies, Scripps Institution of Oceanography, La Jolla, CA 92093, USA

[2] Office of Naval Research, Code 1121CS, 800 N. Quincy St., Arlington, VA 22217, USA

ABSTRACT. Observations from moorings and hydrographic surveys during the Gibraltar Experiment are used to describe the structure in space and time of the internal tide in the strait. By internal tide is meant those fluctuations of the interface (separating inflowing Atlantic from outflowing Mediterranean waters) that have a persistent and demonstrable phase relationship to the barotropic tide. Two modes of fluctuation dominate the variance at semi-diurnal frequency: rising and falling of the interface throughout the strait, which explains about half of the total variance, and fluctuations in the cross-strait slope of the interface, which explains about 25% of the variance. The largest amplitude fluctuations are found at the Camarinal sill. The interface rises and falls approximately in quadrature with the barotropic current, and a kinematic argument for why that should occur is presented. The cross-strait slope of the interface changes approximately in phase with the barotropic tidal currents, corresponding to changes in the vertical shear, in what may be an incomplete geostrophic adjustment in the cross-strait direction.

1. Introduction

Locally generated internal fluctuations, occurring at tidal frequencies within and near the Strait of Gibraltar, contribute several times as much energy to the system as does the mean buoyancy-driven exchange. Interaction of the barotropic tide with the Camarinal sill generates large amplitude fluctuations of the interface between Atlantic and Mediterranean waters. Of these fluctuations, some are resolved into traveling solitary wave packets, some overturn and mix the water column, and some are found to have consistent phase relationships throughout the strait. It is the latter we examine here, and will refer to as the internal tide.

There are two types of interface fluctuations associated with the internal tide: the interface depth increases or decreases, and the cross-strait slope of the interface varies. We will argue that the depth of the interface varies as a result of kinematic requirements associated with the large amplitude barotropic tidal currents, and that the cross-strait slope varies as a result of fluctuations in the vertical shear at tidal frequencies.

L. J. Pratt (ed.), The Physical Oceanography of Sea Straits, 477–491.

2. Description of the Internal Tide from Observations

As no one type of observation is ideal for constructing an adequate description of the internal tide in the strait, we have combined moored time series observations (current, temperature, salinity, and bottom pressure) with hydrographic survey measurements wherever we can demonstrate that the different approaches are consistent. In the Gibraltar Experiment data set, the primary limitation of the moored observations is lack of resolution: both horizontally and within the upper inflow layer. Use of hydrographic observations in the strait is limited principally by aliasing of the semi-diurnal tide. In the present work, we have utilized CTD time series (yoyo) casts, maps constructed from stations taken at the same phase of the semi-diurnal tide and rapid cross-strait surveys to avoid, to some extent, these aliasing problems.

2.1 MEAN INTERFACE GEOGRAPHY

It has long been recognized that there exists a 'mean' structure to the interface: shallower east of the sill, deep west of the sill and with a tilt downward to the south to accommodate the geostrophically balanced buoyancy-driven exchange through the strait (Lacombe and Richez, 1982). This average interface structure is apparent, despite the large amplitude fluctuations in the depth of the interface, particularly near the Camarinal sill, as illustrated in Figure 1, a map constructed from all of the hydrographic data taken in the strait during the Gibraltar Experiment (cruises in November 1985, March, June and September of 1986; [Bray, 1986; Shull and Bray, 1989; Kinder et al. 1986, 1987]).

The average distribution of interface depth was constructed in the following way: the average depth of the salinity interval 37 to 38 was first determined for each station. (The structure of the interface is relatively insensitive to this definition: for instance, defining the interface as 36.9 to 37.1 gives the same result as 37 to 38 for all topics discussed here.) Second, the stations were grouped according to time relative to high water at Tarifa (hereafter HW), independent of season or spring/neap cycle. We chose this differentiation because the largest variances in interface depth, by far, are associated with semi-diurnal fluctuations; spring/neap and seasonal variations, though not negligible for some calculations, are less important in determining interface depth. Also, there are insufficient data to further subdivide the categories without losing significant horizontal resolution. Third, each group of stations corresponding to observations taken within a given hour relative to HW was objectively mapped onto a horizontal grid, using standard techniques and an exponentially decaying correlation scale. (Parameters used were 40 km decay scale and an error variance of 0.03). Finally, all 12 grids were averaged, point by point, to create the map shown in Figure 1.

As a comparison, the data were also divided into rectangular areas within the strait and simply averaged. The patterns derived from the two techniques are indistinguishable, except in the northwest corner where there are very few data. The advantage of the objective mapping technique is that it provides gridded data for each of the hourly maps, facilitating calculations we present later.

2.2 SEMI-DIURNAL FLUCTUATIONS OF THE INTERFACE

Given the average structure of the interface, we can then proceed to examine fluctuations about that average. We will present three different analyses of those fluctuations: first by simply subtracting the average field from each of the hourly maps (Figure 2), second by using an empirical orthogonal function (EOF) decomposition of the CTD-derived hourly maps (Figure 3), and third through an harmonic analysis of the interface fluctuations inferred from moored measurements of temperature and salinity (Figure 4). In general, we will not make a distinction between semi-diurnal and M_2, although we recognize that the latter is only one of several constituents contributing to the semi-diurnal band. Thus, the CTD observations will include all fluctuations occurring within that band, but harmonic analyses will be related specifically to the M_2 constituent; the error associated with neglecting the other components in the strait is small compared to sampling errors and noise from other processes, such as internal waves.

The time sequence of fluctuations illustrated in Figure 2 has several interesting characteristics in common with the harmonic analysis of Figure 4:

- the largest fluctuations are found at the sill;
- fluctuations are larger on the south side of the sill than in the north;

- there is a sense of phase propagation from west to east (e.g., the steady eastward movement of the zero line from -30 km at high water HW to +20 km at HW +5);
- there is a tendency for phase propagation from north to south at the sill (e.g., the intrusion of positive anomaly begins on the northern side of the sill at LW and rapidly moves south). The amplitude of fluctuations overall is larger in the CTD-derived data than for the mooring-derived interface; this may result from inadequate resolution of the upper layer by the moored instruments.

A more compact analysis of the CTD-derived interface fluctuations is shown in the EOF results of Figure 3. In the top panels of Figure 3 we have reproduced the average interface depth map, together with a map of standard deviations of interface depth calculated from the hourly grids. The center panels illustrate the spatial structure of the first and second EOF modes, while the time structure of those modes appears in the lower left panel. For comparison, Figure 4 is reproduced to the same scale in the lower right panel.

The temporal structure of both modes is nearly sinusoidal, with semi-diurnal period. However, there is roughly 90° phase difference between the two. In the strait, the barotropic tidal current lags the surface elevation by roughly 90° (Candela, Winant and Ruiz, 1989), with maximum flood tide occurring 3 hours after HW. The first two EOF modes then correspond approximately to maximum surface elevation (mode 1) and maximum tidal currents (mode 2). This sinusoidal time dependence suggests that the EOF decomposition is usefully describing a geophysical process. The first EOF mode (44% of the variance) has its maximum amplitude in time one hour before high water and its minimum one hour before low water. The spatial structure associated with this mode corresponds to the interface either rising or falling throughout the strait, with maximum amplitude on the southern side of the sill. The second mode (27% of the variance) has its maximum one hour before maximum flood current and its minimum one hour after maximum ebb current relative to Tarifa.

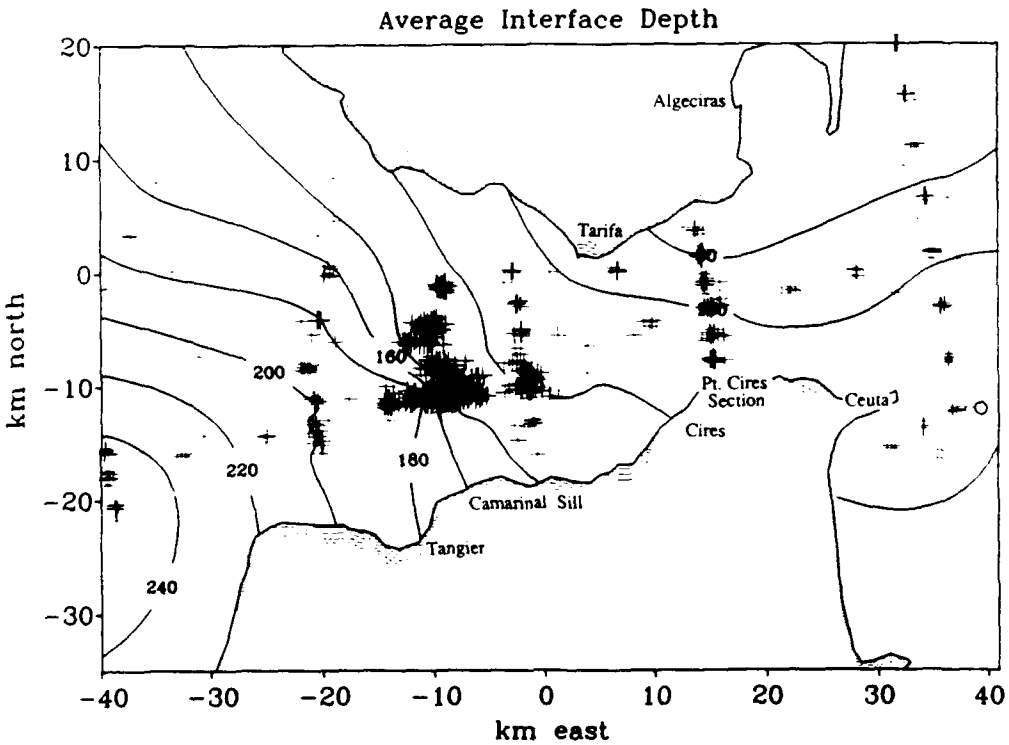

Figure 1. The average interface depth, in meters, throughout the Strait of Gibraltar, based on hydrographic data. Observations used include those from four Gibraltar Experiment cruises. Geographic locations referred to in the text are noted; crosses denote station locations.

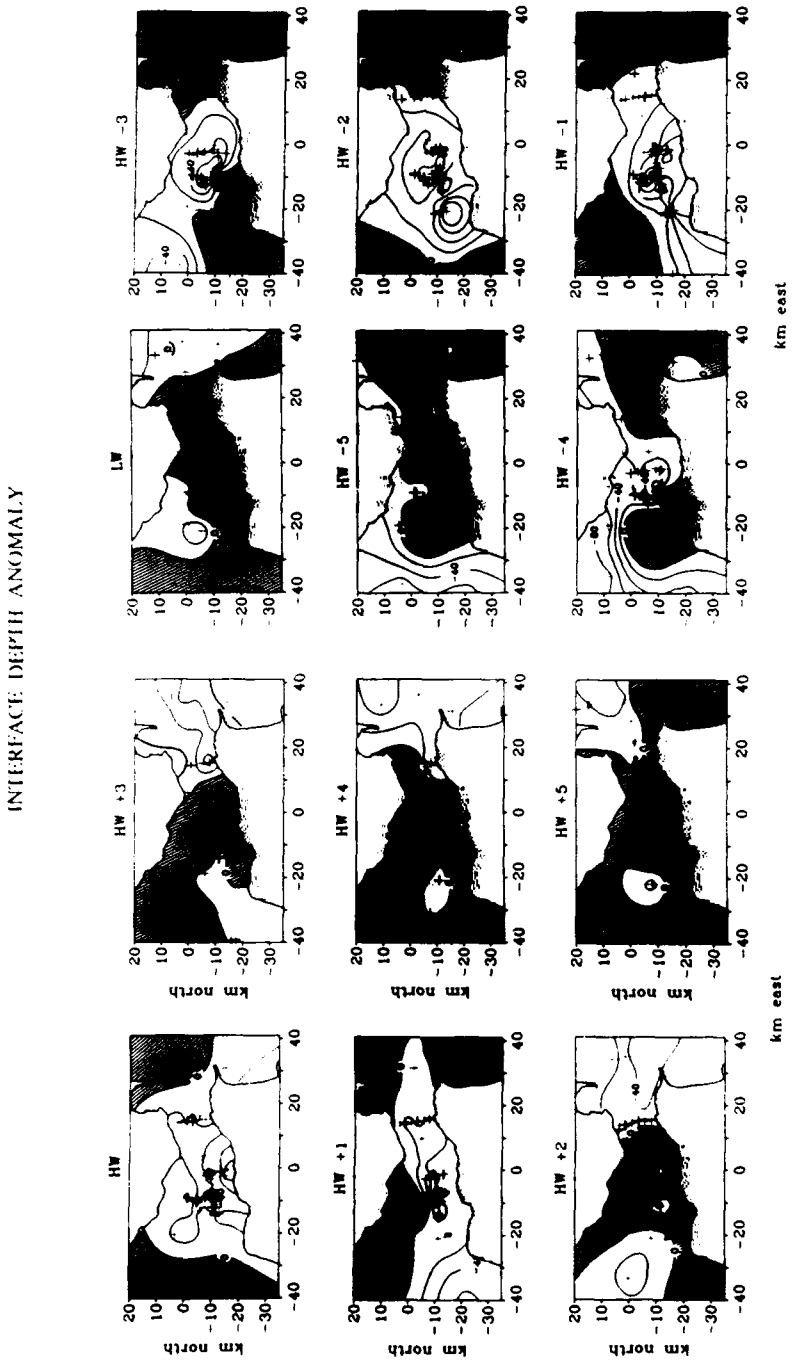

Figure 2. Interface depth anomaly from the average shown in Figure 1, as a function of hours from high water at Tarifa. Depths in meters. Shaded areas represent regions where the interface is deeper than the mean value.

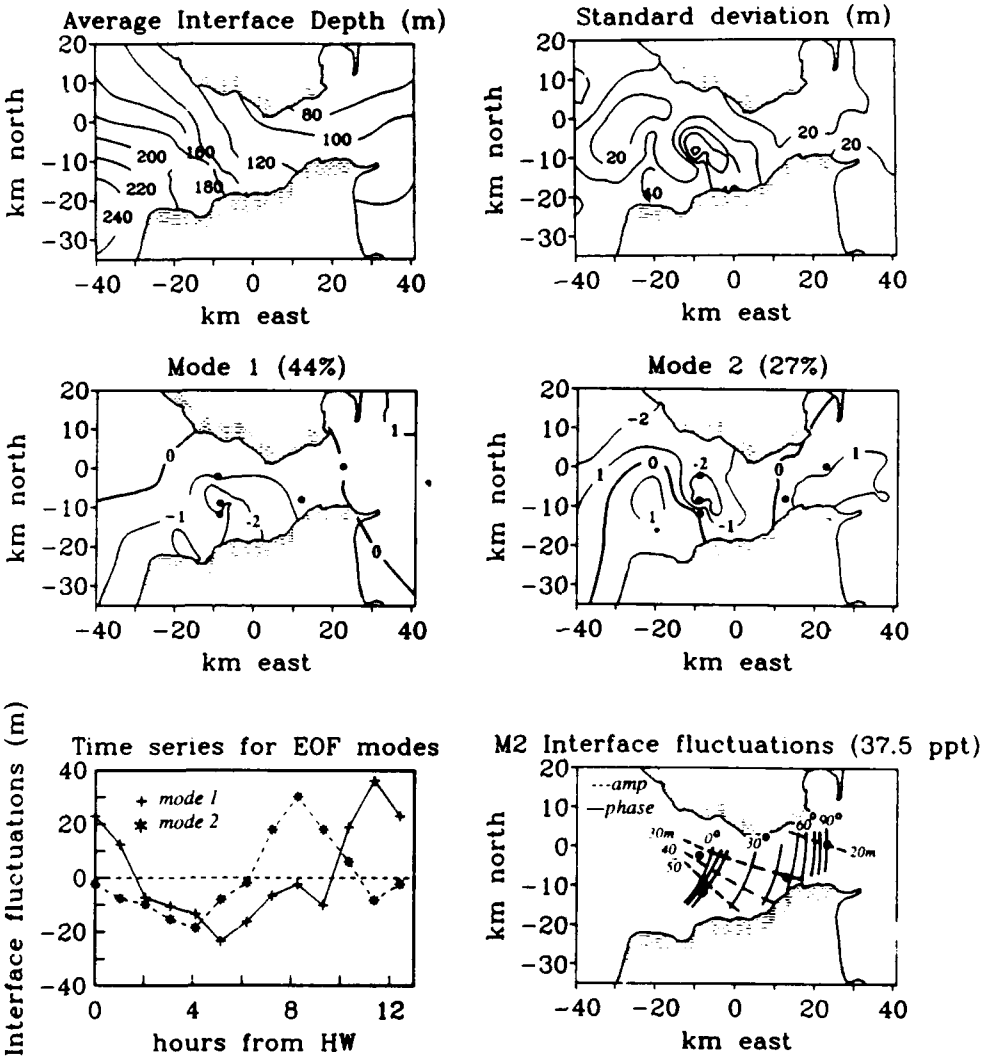

Figure 3. Empirical orthogonal analysis of fluctuations in interface depth as derived from CTD observations. Top panels are average and standard deviation of 12 maps, each corresponding to the horizontal structure of the interface at a given hour relative to HW. Center panels are the spatial structures for modes 1 and 2. Lower left panel shows the time behavior of the two modes, and lower right panel the harmonic analysis of interface depth from Figure 4, reduced to the same scale for comparison with the EOF analysis.

Historically, the surface tide at Tarifa has been used as reference for phase considerations of oceanographic phenomena in the strait. A more general reference would be Greenwich, as is typically used in tidal analyses. For the M_2 surface tide constituent, the phase of Tarifa relative to Greenwich is 41°, and a phase change of 1 hour for M_2 corresponds to 28.9°. Thus, the EOF decomposition implies phases (Greenwich) of 12° for mode 1 and 99° for mode 2.

The traditional, and very useful, description of tides in terms of amplitude (co-range) and phase (co-tide) isopleths is a result of harmonic analysis utilizing a number of observation points. Although this approach has been most often used to describe surface elevations, it is equally applicable to interface elevations. From moored time series of temperature and conductivity at five locations in the strait (Figure 4), the depth of the interface as a function of time was inferred by assuming a vertical salinity profile and interpolating (or extrapolating when the interface was shallower than the top instrument) between the measured points. Here the interface was defined to be the 37.5 salinity surface, or the middle of the range used to obtain the CTD-derived interface.

Despite the limited horizontal resolution, a fairly clear pattern of phase propagation from west to east emerges in Figure 4. There is also a phase propagation from north to south over the sill, with an average value of about 0° (Greenwich), consistent with the first EOF mode of Figure 3. Also consistent is the increase in amplitude from north to south across the sill. (Recall, however, that these two analyses are not directly comparable, in that phase information is treated differently: phase information in the EOF analysis is limited to the time series behavior, so that real spatial variations in phase may be obscured.) Given the 90° (3 hour) phase lag at the eastern end of the strait, one might expect to see more variance in EOF mode 2 at the eastern end than in mode 1. This appears to be the case.

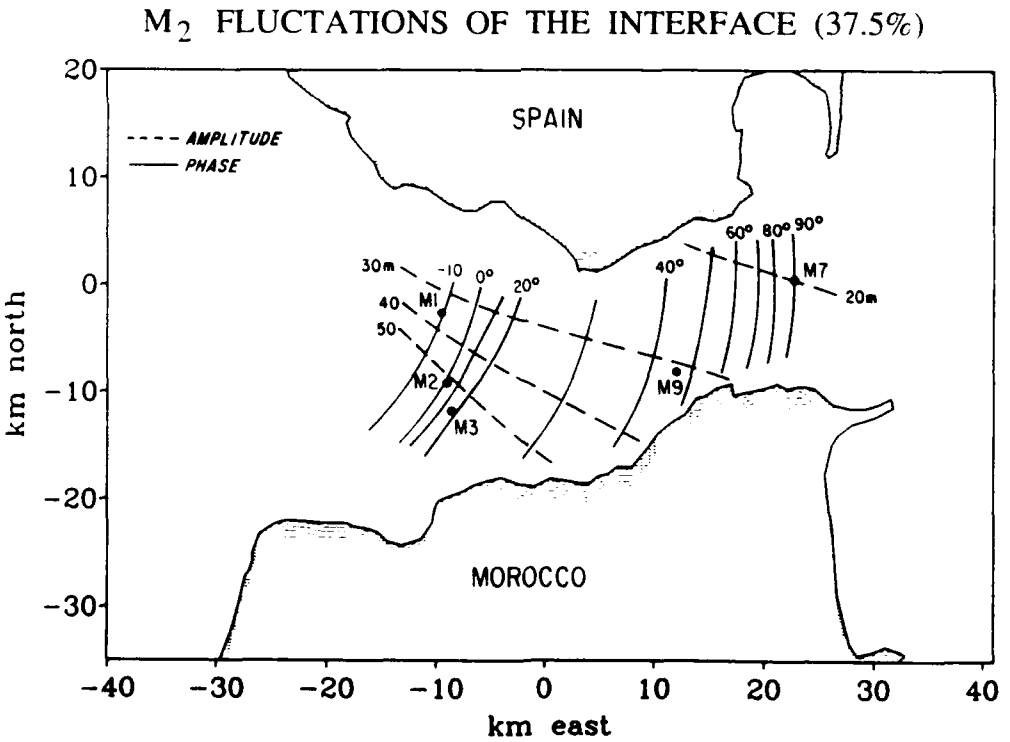

Figure 4. Harmonic analysis (co-tide and co-range lines) for the M_2 constituent of the interface fluctuations as determined from moorings (located by dots).

3. Cross-Strait Structure and Fluctuations

While some useful information about the cross-strait structure of the internal tide can be gleaned from the horizontal maps of the previous section, sufficient observations were taken during the Gibraltar Experiment to allow us to examine cross-strait sections at the main constricting sill, Camarinal, and in the eastern end of the strait near Pt. Cires (see Figure 1 for locations).

3.1 CAMARINAL SILL

Most of the moored observations taken during the experiment were concentrated in the area of the Camarinal sill, the principal vertical constriction for exchange through the strait, with a maximum depth of 320 m. The Tarifa Narrows, however, is the narrowest section, located 15 km east of the sill, and with a depth of about 700 m. Three moorings were located across the sill, on the north (M1), in the center (M2) and at the south (M3) (Figure 5). Mooring M2 was lost after about a month, but is still useful for tidal period analyses. In addition to the moored observations, a large number of CTD time series (yoyo) casts were occupied across and near the sill. Cross-strait sections constructed from these casts are described in detail in Bray and Lacombe (1989) and will not be discussed here.

An EOF decomposition of the cross-strait structure of the observed tidal currents is shown in Figure 5 (spatial structure only for modes 1 and 2). Most of the variance (92.3%) is contained in the first mode, which is barotropic, with some decrease in speed near the bottom. The structure of mode 2 reflects the fluctuations in the vertical shear at tidal frequencies. The time behavior of these two modes is illustrated in Figure 6, along with time series of interface height at M1 and M3 for a 2.5 day period in April of 1986. The top two panels of Figure 6 are the observed interface depths on the south and north sides of the sill. The third panel is the bottom pressure (approximately the surface elevation) measured on the north side of the sill, and is included as an indication of the phase of the surface tide.

In the bottom two panels of Figure 6 the EOF modes of the tidal currents are compared with the cross-strait interface fluctuations: (panel 4) the average depth of the interface (simply the arithmetic average of the interface depths on the north and south sides of the strait) vs the time series of the barotropic tidal current (mode 1); and (panel 5) the cross-strait slope of the interface (calculated as the difference in interface depth from south to north) vs the vertical shear (mode 2). The correspondence between the two time series is remarkably close for both modes. The time lag between the average interface depth and the mode 1 currents is about 3 hours, whereas the interface slope appears to be in phase with the mode 2 currents.

3.2 PT. CIRES SECTION

In November of 1985 a series of 13 hydrographic sections was occupied across the eastern end of the strait, near Pt. Cires (see Figure 1 for section location). The sections were done in two groups: one at spring tides and one at neap tides. Succeeding sections were occupied as quickly as possible, alternating direction of transit each time. One transit, comprising 6 stations, took from 2 to 4 hours to accomplish. We have taken these 13 transits and compiled them into a time series, with 'time' taken to be the midpoint of the interval required by a given transit. Some aliasing of the tide undoubtedly occurs with this approach, but the resultant EOF decomposition is fairly convincing that tidal frequency fluctuations are resolved by these observations.

The average salinity and its standard deviation as determined from the 13 surveys across the Cires section are shown in Figure 7. Note that the interface is shallower to the north (to the right) in the average and that there are regions on either side of the strait where the standard deviation is high, reflecting variations in the slope of the interface. The first two EOF modes calculated for this series of sections have generally sinusoidal, semi-diurnal time behavior. Like the EOF modes shown in Figure 3 for the interface depth as a function of horizontal position in the strait, the first mode in the Cires analysis corresponds to salinity uniformly increasing or decreasing across the strait (in the depth range occupied by the interface). The maximum change occurs at the average depth of the interface, and on the south side of the strait. This salinity fluctuation is equivalent to the interface rising and falling. The time behavior is also similar to that of Figure 3: nearly in phase with the surface elevation, plotted as a dotted line in the time series plot

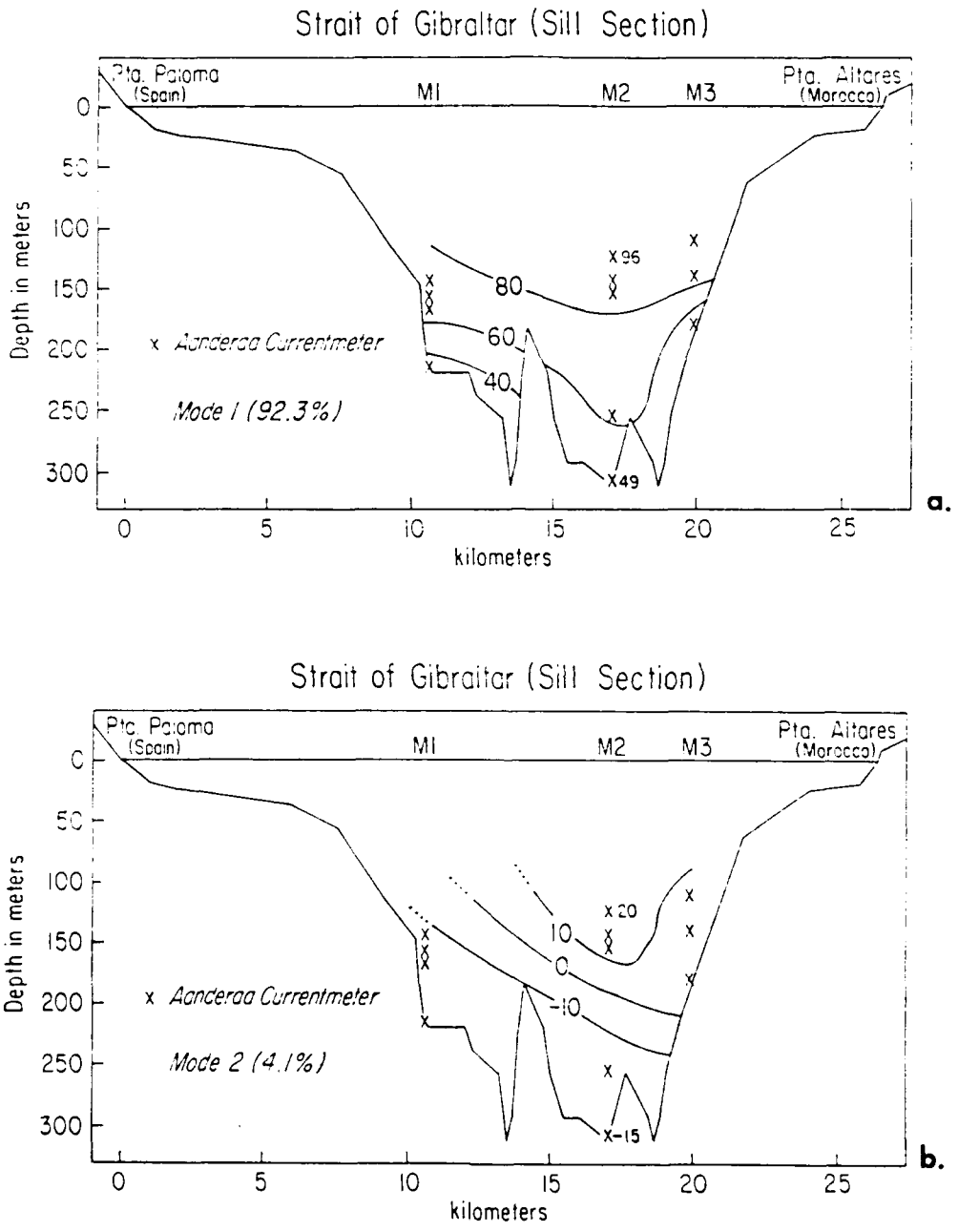

Figure 5. Spatial structure of the first two modes of the tidal currents ($\sigma > 0.5$ cpd) from a section across the sill (north is on the left). Contours are in cm sec^{-1}. (Redrawn from Candela, Winant, and Ruiz, 1989).

for mode 1. The phase difference between surface elevation and interface depth has changed, however, and the surface here leads the interface by about 2 hours, whereas at the sill the interface leads the surface by 1 hour. This spatial phase shift is consistent with the harmonic analysis shown in Figure 4.

Mode 2 of the Cires section is less sinusoidal in time, but is at least partly correlated with maximum tidal current (indicated here by phase-shifting the tidal elevation by 3 hours, the observed phase difference between elevation and current in the strait). The spatial structure of mode 2 corresponds to changing the slope of the interface: for example, when salinity increases on the north side, it decreases on the south, reflecting an increased tilt.

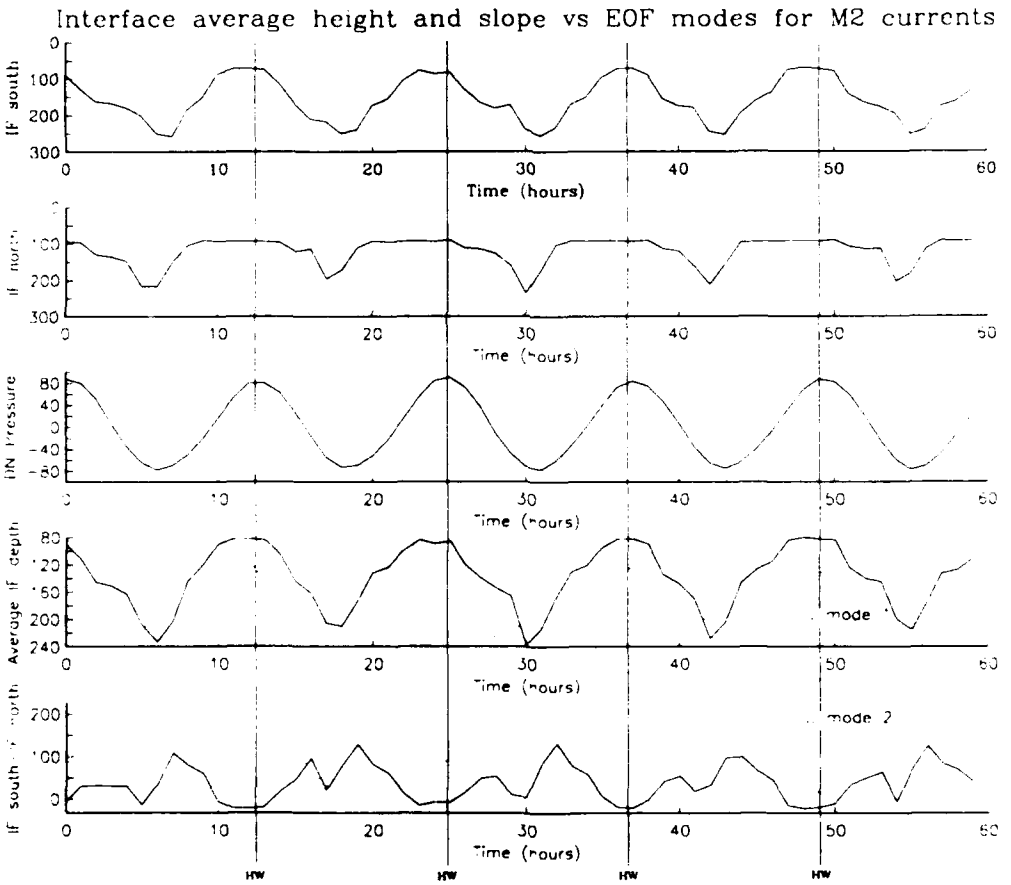

Figure 6. Interface depths in meters from moored data on the south (top panel) and north (second panel); bottom pressure from the sensor at DN, corresponding to the surface elevation (third panel). In the lower two panels: comparison of the average interface depth (solid line) and the time series of mode 1 from Figure 5 (dotted line); and comparison of the interface difference (solid line) and the time series of mode 2 from Figure 5 (dotted line).

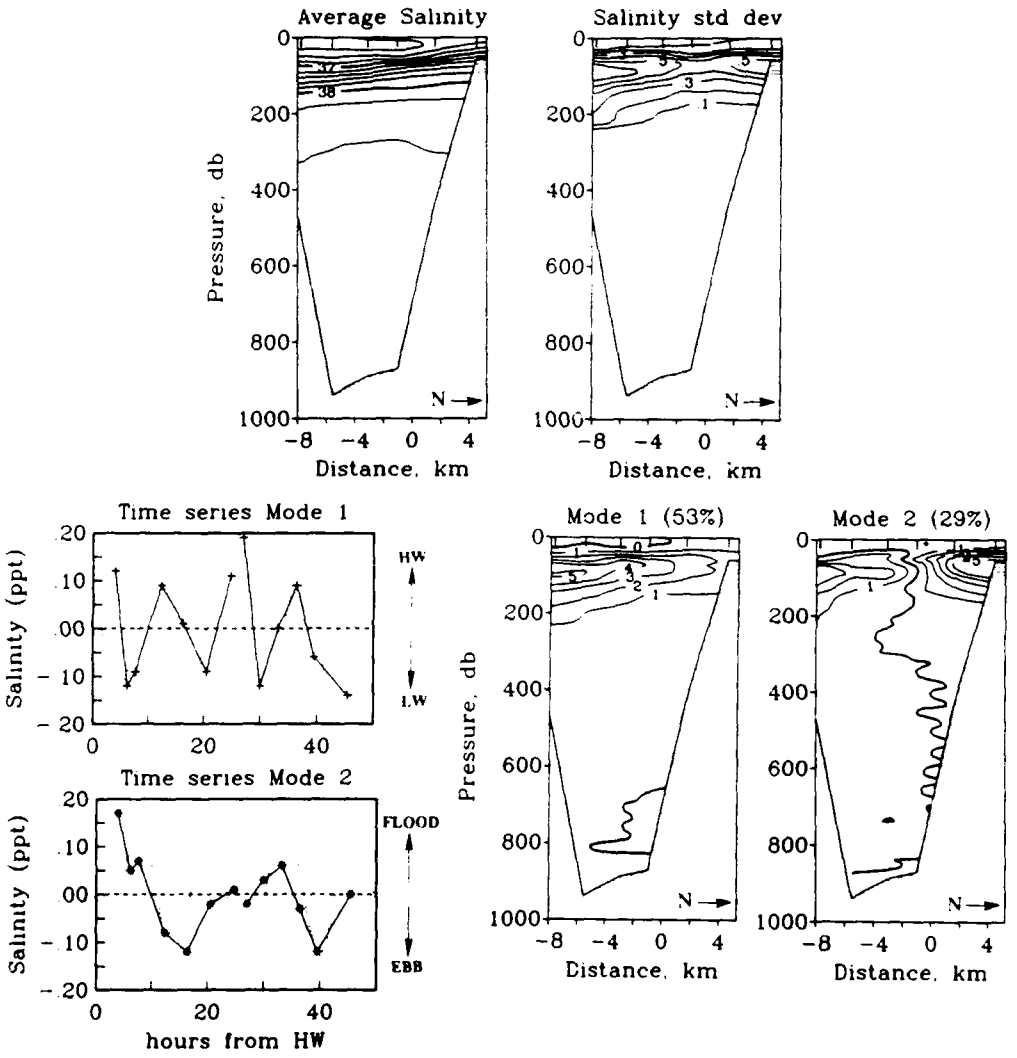

Figure 7. Empirical orthogonal analysis of the Cires hydrographic sections. Top panels are average and standard deviations of 13 cross-strait sections occupied in rapid succession. Center panels illustrate the temporal and spatial behavior of the first two modes. For comparison in the time series plots, surface elevation is plotted as a dotted line with mode 1, and surface elevation shifted by 90°, to represent maximum current, is plotted as a dotted line with mode 2.

4. Discussion

The overall structure of the internal tide in the strait can be summarized as follows. The surface elevation of the M_2 tide is nearly in phase throughout the strait. The barotropic tidal currents are also nearly in phase throughout the strait (except in the upper layer at the eastern end of the strait), and 90° out of phase with the surface elevation, with maximum flood current following high water. The elevation of the interface has fixed phase relative to either maximum current or surface elevation at the Camarinal sill and the Pt. Cires section, though with different lags in the two locations. At the sill, the interface leads the surface elevation by about an hour, while at Cires the interface lags the surface elevation by about 2 hours. In addition to rising and falling, the interface slope also changes in phase with the tidal frequency vertical shear fluctuations at the sill, and in phase with the tidal current at the Cires section. Based on the EOF analyses of CTD data throughout the strait and across the Pt. Cires section, roughly 50% of the total variance is associated with the rising and falling of the interface, while another 25% is associated with the change in cross-strait interface slope.

The 3-hour phase difference observed between the sill and the eastern end of the strait in the interface fluctuations corresponds to a propagation speed of about 3 m sec^{-1}, 2 to 3 times the expected phase speed of an internal wave travelling along the interface. It is likely, therefore, that the response of the interface in the eastern strait results from a combination of local response to local tidal currents and westward propagation of some type of adjustment occurring east of the sill.

Why should the interface rise and fall in phase with the surface elevation? The simplest argument we can construct is kinematic, involving continuity of mass in two layers of different depths and significant along-strait depth variation, when a large barotropic current is imposed, as illustrated schematically in Figure 8. In the limit of the lower layer depth going to zero west of the strait and the upper layer vanishing east of the strait, and assuming no flow through the interface, the interface must act as deformable surface to accommodate the additional mass flux associated with the barotropic tidal currents. The rate of change of the depth of the interface will be maximum when the tidal current is maximum, and the interface will reach its deepest and shallowest points at slack tides (low water and high water, respectively). Because the surface elevation and tidal currents in the strait are in quadrature, the depth of the interface is, coincidentally, in phase with the surface elevation. However, in this argument, it is the tidal current that drives fluctuations of the interface. In addition to the vertical constraint imposed by the sill, there is a horizontal constraint imposed by the Tarifa Narrows, that will have a significant effect on the continuity argument. It is therefore necessary to consider the convergence and divergence of the transport rather than simply the velocity field in constructing the governing equation here. Let $W(x)$ be the width of the strait, $h(x, t)$ the height of either layer, $u(t)$ the barotropic tidal current, and x and t along-strait distance and time. The continuity equation is then:

$$\frac{\partial Wh}{\partial t} = \frac{\partial (Whu)}{\partial x} \tag{1}$$

Candela, Winant and Ruiz (1989) estimated from moored observations at the sill and at the eastern end of the strait the time rate of change of the lower layer volume enclosed by those moorings and the difference in transports in the lower layer through the two sections. This corresponds to evaluating the two terms of equation (1), integrated in x, as a function of time:

$$\int_{x_1}^{x_2} W \frac{\partial h}{\partial t}\, dx = Whu\,|_{x_1} - Whu\,|_{x_2} \tag{2}$$

The two time series were found to be significantly correlated at the 99% confidence level, and the comparison is shown in Figure 9. The agreement between these time series suggests that the kinematic argument that the interface rises and falls in order to compensate the additional mass introduced into the system by the tidal currents is sound.

KINEMATICS OF TIDAL FLUCTUATIONS OF THE INTERFACE

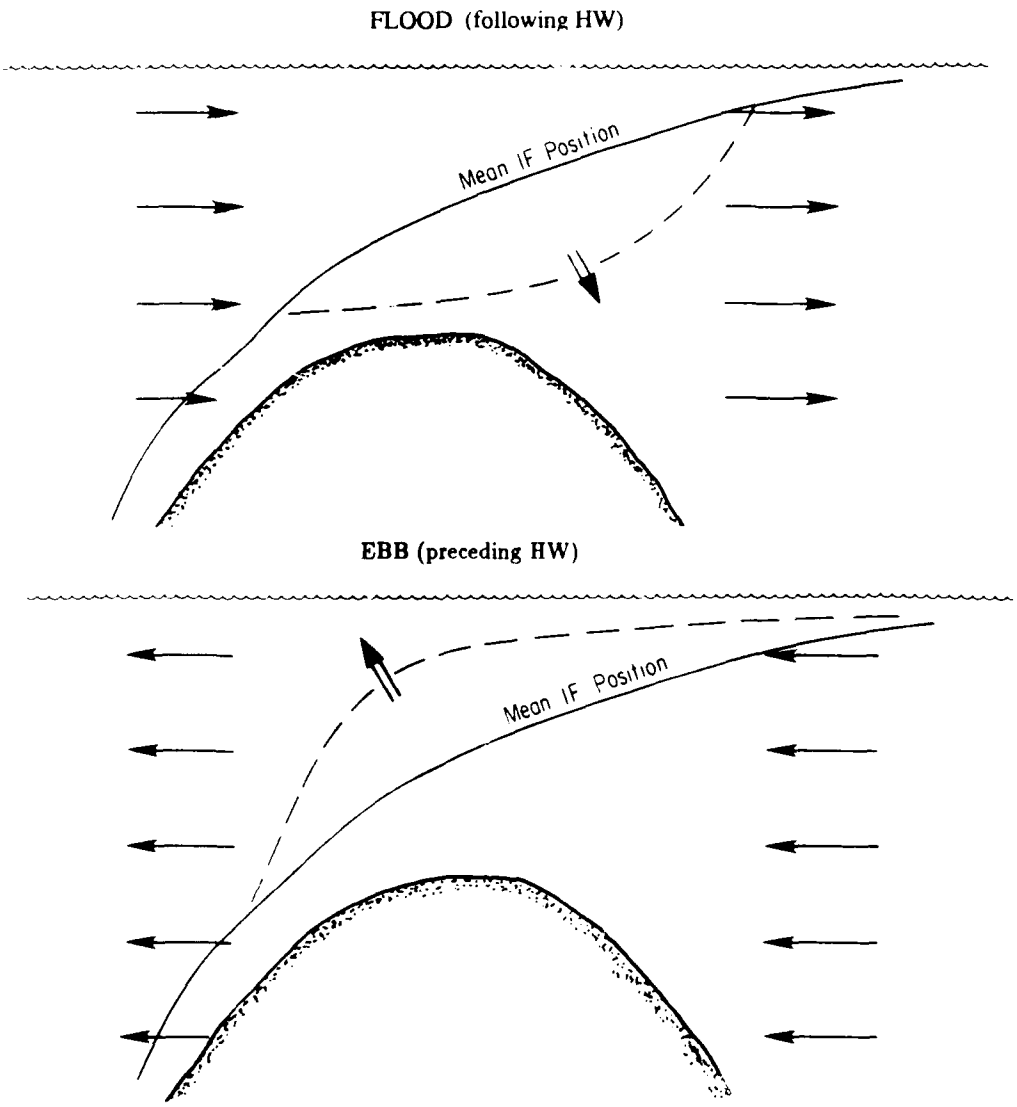

Figure 8. Schematic of the effect of a uniform barotropic current acting upon a two layer system with very different layer depths east and west of the sill, and significant change in layer depth moving along the strait.

Why should fluctuations in the slope of the interface be associated with vertical shear at tidal frequencies? The answer to this question at low frequencies is fairly clear: a geostrophic balance is established, and the cross-strait slope of the interface accommodates a known vertical shear. In the case of an oscillatory flow, at higher frequency, there may not be sufficient time for the mass field to adjust to a geostrophic balance before the flow field changes, or even reverses. The time required for adjustment is the travel time for an internal wave to cross the strait: $\sqrt{g'h}$, or about 3 hours for the Camarinal sill. This time period corresponds to one-quarter of a semi-diurnal period, so that it is unlikely that full adjustment ever occurs. However, there does appear to be a partial adjustment, and, as the vertical shear produced at tidal frequencies is not negligible, the variance associated with changing cross-strait slope of the interface is a significant contribution to the total.

Throughout this paper we have limited the discussion to the semi-diurnal frequency band. However, Candela, Winant and Bryden (1989) have shown that important low frequency fluctuations in transport through the strait are both barotropic and associated with in-phase fluctuations of the interface. It is of interest, then, to examine the similarities between the high frequency barotropic flows discussed here and lower frequency phenomena. Although a thorough discussion is beyond the scope of this paper, we offer a summary figure. The left panel of Figure 10 illustrates the coherence between the first current EOF modes at the sill, calculated using all frequency bands, not just the M_2, and the average interface depth; and the right panel illustrates the coherence between the second mode and the interface slope, or difference, across the strait. The spatial structures of these two modes, though not shown, are similar to the tidal modes seen in Figure 5: mode 1 is associated with barotropic current fluctuations, and mode 2 with vertical shear.

The average interface depth and the mode 1 currents are coherent at the 95% confidence level from the lowest frequencies, corresponding to about 40 days, through the diurnal band, and with significant peaks at semi-diurnal and higher frequencies. The phase changes from approximately zero at low frequencies to 90° at the semi-diurnal and higher frequencies. There is less coherence at low frequency between mode 2 and interface slope, with an important exception at the fortnightly period (14 days). Coherence is high again at diurnal and higher frequencies. The phase relationship, unlike the mode 1 case, does not appear to change with frequency, but remains at zero for all frequencies where the coherence is significantly different from zero.

From this summary figure, we may surmise that low frequency barotropic fluctuations do not behave in the same way as tidal barotropic fluctuations: the phase relationship between current and interface depth is zero, rather than 90°, and there is no apparent tendency for the cross-strait slope of the interface to change, or equivalently, for vertical shear to be generated. Fortnightly fluctuations also behave differently than do those in the semi-diurnal band, in that there is again zero phase lag between the current and the interface depth fluctuations, as well as significant coherence between cross-strait interface slope and shear.

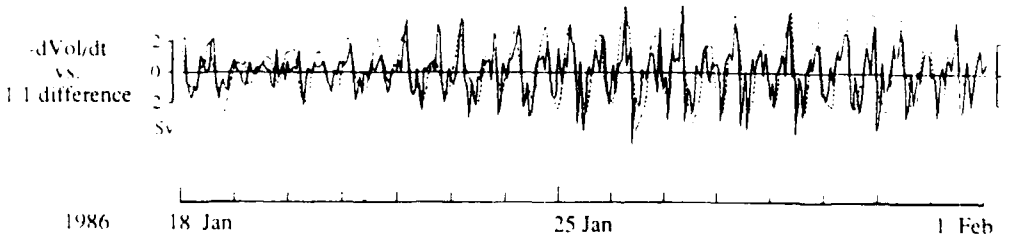

Figure 9. Comparison of the change in volume with time (solid line) with the difference in transport in the lower layer at either end of the volume (dotted line). The volume is defined by the Camarinal sill on the west and mooring M7 at the eastern end of the strait (see Figure 4 for mooring locations), the (time-varying) interface depth and the bottom of the strait. (Redrawn from Candela, Winant, and Ruiz, 1989).

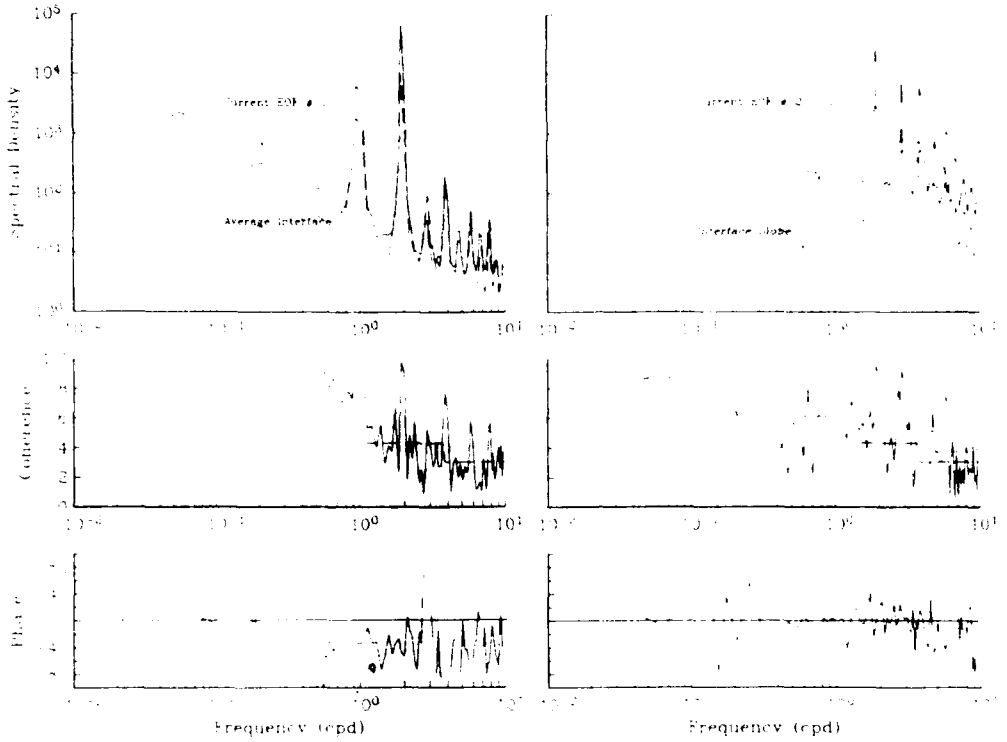

Figure 10. Spectra and coherence and phase estimates for (left panels) current EOF mode 1 and cross-strait average interface depth, and (right panels) current EOF mode 2 and cross-strait interface slope. Dashed lines are 95% confidence limits.

5. Acknowledgements

The observations discussed in this paper were collected during the Gibraltar Experiment, under the auspices of the United States Office of Naval Research. We are grateful to Harry Bryden and Dale Pillsbury for permission to use the moored current observations they collected during the experiment. NAB was supported under ONR contract #N00014-85-C-0407 during the acquisition and analysis of observations and the preparation of this manuscript. THK received support from ONR under Code 422CS program element 61153N, and CDW and JC from ONR contract #N00014-85-C-0223. Special thanks go to Joan Semler and Michael Clark for their painstaking preparation of the camera-ready final version of the paper. As always, we are indebted to the many people who made it possible to acquire observations at sea, especially in as challenging an environment as the Strait of Gibraltar.

6. References

Bray, N. A. (1986) Gibraltar experiment CTD data report, March-April 1986, USNS *Lynch, SIO Ref. 86-21*, 212 pp., Scripps Inst. of Oceanogr., La Jolla, Calif., USA.

Bray, N. A., and H. Lacombe (1989) Tidal modulation of water mass exchange in the Strait of Gibraltar. In preparation.

Candela, J., C. D. Winant, and H. L. Bryden (1989) Meteorologically forced subinertial flows through the Strait of Gibraltar, accepted by *J. Geophys. Res.*

Candela, J., C. D. Winant, and A. Ruiz (submitted 1989) Tides in the Strait of Gibraltar, *J. Geophys. Res.*

Kinder, T. H., D. A. Burns, and R. D. Broome (1986) Hydrographic measurements in the Strait of Gibraltar, November 1985, *Naval Ocean Research and Development Activity Report 141*, 332 pp.

Kinder, T. H., D. A. Burns, and M. R. Wilcox (1987) Hydrographic measurements in the Strait of Gibraltar, June 1986, *NORDA Tech. Note 378-1* (Appendix), 355 pp.

Lacombe, H., and C. Richez (1982) The regime of the Strait of Gibraltar, in *Hydrodynamics of Semi-enclosed Seas*, edited by J. C. J. Nihoul, pp. 13-74, Elsevier, Amsterdam.

Shull, S., and N. A. Bray (1989) Gibraltar Experiment CTD data report: September-October 1986, USNS *Lynch*. In preparation.